Communications on Applied Nonlinear Analysis
ISSN: 1074-133X
Vol 31 No. 6s (2024)

# Influence of Cattaneo-Christov Heat Flux Model Rotating Maxwell Nanofluid with MHD and Double Stratification Across a Bidirectional Stretching Surface

**Kanchana M [1] ,Lakshmi R [2] , R.Vijayakumar[3]**

[1]Research scholar, Department of Mathematics, PSGR Krishnammal College for Women, Coimbatore – 641004, Tamil Nadu, India

[2]Assistant Professor, Department of Mathematics, PSGR Krishnammal College for Women, Coimbatore – 641004, Tamil Nadu, India E-mail: lakshmir@psgrkcw.ac.in

[3] Mathematics Section, FEAT, Annamalai University,Annamalainagar – 608002, India.

Department of Mathematics, Periyar Arts College,Cuddalore, Tamil Nadu,India.

E-mail: rathirath_viji@yahoo.co.in

***Article History:***

***Received:*** *13-06-2024*

***Revised:*** *11-07-2024*

***Accepted:*** *02-08-2024*

**Abstract:**

In this research, New homotopy analysis method for solving the fractional (2+1) D and (3+1) D non-linear Schrödinger equations by Elzaki. To solve these equations , the Elzaki transform is applied jointly to the Homotopy analysis method (HAM). This has proved efficient in tackling fractional calculus and nonlinear dynamics since correct solutions are offered and they converge at a faster rate. The accuracy of the proposed technique has been corroborated by analyzing various examples for which the latter were used for solving high-dimensional non-linear Schrodinger equation, which indicates that the technique is quite resilient as well as efficient; thus, making it an effective tool in theoretical physics and other applied sciences.

**Keywords**: Maxwell nanofluid, Rotating, Cattaneo-Christov heat flux model, Magnetic field, double stratification.

## 1. Introduction

Nanofluids are attempting to develop additional ways to enhance thermal system heat transfer efficiency. Applications of nanofluids are numerous in industrial, and cooling systems like aerodynamics, pipe and valves, electronic battery, air conditioning, ventilations, medicine, power and chemical engineering, and others. Metallic surface is used to construct fittings, reflectors, surface coatings and as a protector in areas where heat radiates. With this surface, the fluid of nanoparticles work as a cooling substance to reduce the heat in various industrial applications. The flow of a Maxwell nanofluid including gyrotactic microorganisms with a heat source/sink and a magnetic field is studied in three dimensions via a stretching surface by Aamir Ali. Convective heat transfer conditions with exponentially stretching sheet for rotating flow of nanofluids were discussed and compared by Ahmad. In rotating incompressible Maxwell nanofluid with CC-Model, chemical reaction and gyrotactic micro-organisms are discussed over a Riga plate. MHD rotating flow of Maxwell and tangent hyperbolic nanofluid with CC-Model over a bidirectional stretching sheet are considered and solved numerically by using finite element analysis.

Fouzia Rehman considered single and multi-walls in micropolar nanofluid to the base fluid with MHD and convective conditions within the parallel rotating plates. Hassan Waqas motivated to improve the heat transfer on nanofluid and hybrid nanofluid flow between rotating plates. Hayat elaborated stretching surface exponentially along with Brownian motion and thermophoresis in the rotating Maxwell fluid flow. Influence of thermal radiation, Iskander Tlili reveals the effect on Maxwell fluid and entropy analysis. Mustafa and Muhammed Naveed Khan examined the variable thermal conductivity by applying CC-Model in the rotating Maxwell fluid. In Muhammad Awais revealed the features, properties of nanofluid to provide the heat transfer performance. Effect of activation energy on rotating Maxwell fluid with double stratification conditions by comparing the linear and exponential stretching surface.

Rahimah Jusoh suggested convective boundary conditions over a stretching/shrinking surface on Maxwell fluid to analyze the heat transfer rate. Ramaiah and Shafique discussed MHD rotating nanofluid with chemical reaction and activation energy by using CC-Model. Considering the solid permeable plate parallel to the stretching surface to analyze the fluid motion effects through various nanoparticles in a rotating frame. Maxwell fluid flow with double stratification, thermal radiation and magnetic field considered by Tariq Hussain. Hayat discussed the rotating flow of Maxwell nanofluid with thermophoresis and Brownian motion, and extend to convective Darcy-Forchheimer with porous medium. Wang explored Maxwell fluid with bio-convective flow by using stretching surface in exponential form with slip effect. Wasim Jamshed investigated Maxwell nanofluid with its properties by comparing the fluids to reveal the boundary layer thickness. Muhammad Ramzan illustrated Maxwell nanoliquid with gyrotactic micro-organisms and heat source/sink on Newtonian heating.

Here, aforementioned studies and detailed review of literature on rotating Maxwell nanofluid by linearly and exponentially stretching surface with various boundary conditions and heat transfer models. Therefore, the aim of this paper to explore the Maxwell condition to the MHD nanofluid flow due to rotating frame across a bidirectional stretching surface. Solving this paper numerically by bvp5c in MATLAB technique which represents quantitative values of Nusselt and Sherwood parameter, and graphs for velocity, thermal and concentration profiles by highlights the model to various impacts of implanted parameters.

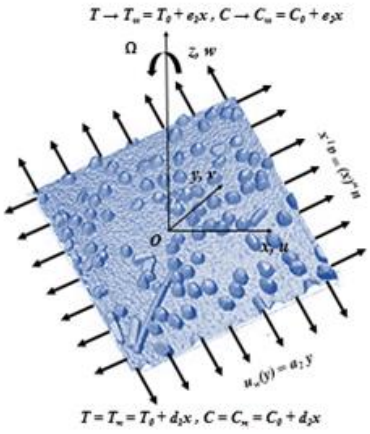


Figure 1. Schematic configuration of the problem

## 2. Mathematical demonstration

Consider the steady, incompressible, three-dimensional rotating Maxwell fluid flow across bi-directional stretching surface with double stratification and magnetic strength. The metal sheet is stretched along x and y directions, the fluid motion is in the path of z-axis which is normal to the surface and it has constant angular velocity ω (say). The motion of fluid is on the z direction which is perpendicular to it and it resides at $z \leq 0$. The stretching velocities of the fluid flow directions are $u_w = a_1x$ (x-direction) and $u_w = a_2y$ (y-direction), ($a_1$, $a_2$ are positive real numbers). With the use of CC model, the equation of energy is updated to simulate thermal impacts. Velocity field $V = (u_1, v_1, w_1)$ is considered to this problem and, while surface temperature and concentration is denoted by $T_w$ and $C_w$, then the ambient temperature and concentration is $T_\infty$ and $C_\infty$ respectively in Figure 1. Governing equations of the considered problem as follows:

$$\frac{\partial u_1}{\partial x}+\frac{\partial v_1}{\partial y}+\frac{\partial w_1}{\partial z}=0 \tag{1}$$

$$u_1\frac{\partial u_1}{\partial x}+v_1\frac{\partial u_1}{\partial y}+w_1\frac{\partial u_1}{\partial z}-2\omega v_1=\frac{\mu_{nf}}{\rho_{nf}}\frac{\partial^2 u_1}{\partial z^2}-\lambda_1\left[u_1^2\frac{\partial^2 u_1}{\partial x^2}+v_1^2\frac{\partial^2 u_1}{\partial y^2}+w_1^2\frac{\partial^2 u_1}{\partial z^2}+2u_1v_1\frac{\partial^2 u_1}{\partial x\partial y}+2v_1w_1\frac{\partial^2 u_1}{\partial y\partial z}\right.$$

$$\left.+2u_1w_1\frac{\partial^2 u_1}{\partial x\partial z}-2\omega\left(u_1\frac{\partial v_1}{\partial x}+v_1\frac{\partial v_1}{\partial y}+w_1\frac{\partial v_1}{\partial z}\right)+2\omega\left(v_1\frac{\partial u_1}{\partial x}-u_1\frac{\partial u_1}{\partial y}\right)-\frac{\sigma_{nf}B_0^2}{\rho_{nf}}\left(u_1+\lambda_1w_1\frac{\partial u_1}{\partial z}\right)\right] \tag{2}$$

$$u_1\frac{\partial v_1}{\partial x}+v_1\frac{\partial v_1}{\partial y}+w_1\frac{\partial v_1}{\partial z}+2\omega u_1=\frac{\mu_{nf}}{\rho_{nf}}\frac{\partial^2 v_1}{\partial z^2}-\lambda_1\left[u_1^2\frac{\partial^2 v_1}{\partial x^2}+v_1^2\frac{\partial^2 v_1}{\partial y^2}+w_1^2\frac{\partial^2 v_1}{\partial z^2}+2u_1v_1\frac{\partial^2 v_1}{\partial x\partial y}+2v_1w_1\frac{\partial^2 v_1}{\partial y\partial z}\right.$$

$$\left.+2u_1w_1\frac{\partial^2 v_1}{\partial x\partial z}-2\omega\left(u_1\frac{\partial u_1}{\partial x}+v_1\frac{\partial u_1}{\partial y}+w_1\frac{\partial u_1}{\partial z}\right)+2\omega\left(v_1\frac{\partial v_1}{\partial x}-u_1\frac{\partial v_1}{\partial y}\right)-\frac{\sigma_{nf}B_0^2}{\rho_{nf}}\left(v_1+\lambda_1w_1\frac{\partial v_1}{\partial z}\right)\right] \tag{3}$$

$$u_1\frac{\partial T}{\partial x}+v_1\frac{\partial T}{\partial y}+w_1\frac{\partial T}{\partial z}=\frac{k_{nf}}{(\rho c_p)_{nf}}\frac{\partial^2 T}{\partial z^2}-\lambda_2\left[u_1^2\frac{\partial^2 T}{\partial x^2}+v_1^2\frac{\partial^2 T}{\partial y^2}+w_1^2\frac{\partial^2 T}{\partial z^2}+2u_1v_1\frac{\partial^2 T}{\partial x\partial y}+2v_1w_1\frac{\partial^2 T}{\partial y\partial z}+2u_1w_1\frac{\partial^2 T}{\partial x\partial z}\right.$$

$$\left.+\left(u_1\frac{\partial u_1}{\partial x}+v_1\frac{\partial u_1}{\partial y}+w_1\frac{\partial u_1}{\partial z}\right)\frac{\partial T}{\partial x}+\left(u_1\frac{\partial v_1}{\partial x}+v_1\frac{\partial v_1}{\partial y}+w_1\frac{\partial v_1}{\partial z}\right)\frac{\partial T}{\partial y}+\left(u_1\frac{\partial w_1}{\partial x}+v_1\frac{\partial w_1}{\partial y}+w_1\frac{\partial w_1}{\partial z}\right)\frac{\partial T}{\partial z}\right] \tag{4}$$

$$u_1\frac{\partial C}{\partial x}+v_1\frac{\partial C}{\partial y}+w_1\frac{\partial C}{\partial z}=D\frac{\partial^2 C}{\partial z^2} \tag{5}$$

With associated boundary conditions,

$$\text{At } z=0, u_1=a_1x, v_1=a_2y, w_1=0, T_w=T=d_1x+T_0,\ C_w=C=d_2x+C_0$$

$$\text{As } z\to\infty, u_1\to 0, v_1\to 0, T\to T_\infty=T_0+e_1x, C\to C_\infty=C_0+e_2x \tag{6}$$

Thermophysical properties for Maxwell nanofluid.

$$\mu_{nf}=\frac{\mu_{bf}}{(1-\phi)^{2.5}},\ (\rho c_p)_{nf}=(1-\phi)(\rho c_p)_{bf}+\phi(\rho c_p)_{np},\ \frac{\rho_{nf}}{\rho_{bf}}=(1-\phi)+\phi\frac{\rho_{np}}{\rho_{bf}},$$

$$\frac{\sigma_{nf}}{\sigma_{bf}}=\left[1+\frac{3\left(\frac{\sigma_{np}}{\sigma_{bf}}-1\right)\phi}{\left(\frac{\sigma_{np}}{\sigma_{bf}}+2\right)-\left(\frac{\sigma_{np}}{\sigma_{bf}}-1\right)\phi}\right],\quad \frac{k_{nf}}{k_{bf}}=\left[\frac{(k_{np}+2k_{bf})-2\phi(k_{bf}-k_{np})}{(k_{np}+2k_{bf})+\phi(k_{bf}-k_{np})}\right] \tag{7}$$

Here, $\phi$ is nanoparticle volume fraction. Also, the subscripts bf, np and nf represents basefluid, nanoparticle and nanofluid.

The dimensionless transformation of the mathematical model are:

$$u_1 = a_1 x f'(\zeta),\ v_1 = a_1 y g'(\zeta),\ w_1 = -\sqrt{a_1 \upsilon}[f(\zeta)+g(\zeta)],$$
$$\zeta=\sqrt{\frac{a_1}{\upsilon}}z,\ \theta(\zeta)=\frac{T-T_\infty}{T_w-T_0},\ \phi(\zeta)=\frac{C-C_\infty}{C_w-C_0} \tag{8}$$

By this transformation, Eqn (1) satisfies. While Eqs (2) to (5) are:

$$f'''\left(\frac{1}{\Pi_1\Pi_2}-\beta_1(f+g)^2\right)-f'^2+2\lambda\beta_2 g'+2\beta_1 f'f''(f+g)+(f+g)f''+2\beta_1\beta_2\lambda\left(g'^2-(f+g)g''-f'g'\right)$$

$$-\frac{\Pi_4}{\Pi_2}M\left(f'-\beta_1(f+g)f''\right)=0 \tag{9}$$

$$g'''\left(\frac{1}{\Pi_1\Pi_2}-\beta_1(f+g)^2\right)+g''(f+g)-g'^2-2\beta_1(f+g)g'g''-2\frac{\lambda}{\beta_2}f'+2\frac{\beta_1\lambda}{\beta_2}\left((f+g)f''-f'^2+f'g'\right)$$

$$+\frac{\Pi_4}{\Pi_2}M\left(\beta_1(f+g)g''-g'\right)=0 \tag{10}$$

$$\theta''\left(\frac{\Pi_5}{\Pi_3\,\mathrm{Pr}}-\beta_3(f+g)^2\right)+(f+g)\theta'(1-\beta_3(f'+g'))=0 \tag{11}$$

$$\Phi''+(f+g)Sc\Phi'=0 \tag{12}$$

Subjected to the boundary conditions are:

$$\text{At } \zeta=0,\quad f'=1,\quad g'=S,\quad \theta=1-S_1,\quad \Phi=1-S_2$$

$$\text{As } \zeta\to\infty,\quad f'=g'=0,\quad \theta=0,\quad \Phi=0 \tag{13}$$

Where $\Pi_i$′s, i = 1, 2…5 in Eqs (9) - (12) shows the Thermophysical properties for the Maxwell nanofluid,

$$\Pi_1=(1-\phi)^{2.5},\quad \Pi_2=\left(1-\phi+\phi\frac{\rho_{np}}{\rho_{bf}}\right),\quad \Pi_3=\left(1-\phi+\phi\frac{(\rho c_p)_{np}}{(\rho c_p)_{bf}}\right),$$

$$\Pi_4=\left[1+\frac{3\left(\frac{\sigma_{np}}{\sigma_{bf}}-1\right)\phi}{\left(\frac{\sigma_{np}}{\sigma_{bf}}+2\right)-\left(\frac{\sigma_{np}}{\sigma_{bf}}-1\right)\phi}\right],\quad \Pi_5=\left[\frac{(k_{np}+2k_{bf})-2\phi(k_{bf}-k_{np})}{(k_{np}+2k_{bf})+\phi(k_{bf}-k_{np})}\right]$$

The parameters are defined here by $\beta_1 = \lambda_1 a_1$ is the Deborah relaxation number, $M = \sigma_{bf} B_0^2 / \rho_{bf} a_1$ magnetic parameter, $\lambda = \omega / a_1$ rotation parameter, $\beta_2 = \lambda_2 a_1$ Deborah retardation number, $S=a_2/a_1$ stretching ratio, $Sc=\upsilon_{bf}/D$Schmidtnumber, $Pr=\upsilon_{bf}(\rho c_p)_{bf}/ k_{bf}$ Prandtl number, $S_2=e_2/d_2$ concentration stratification and $S_1=e_1/d_1$ thermal stratification.

We can use Fourier and Fick's law to determine what Nusselt and Sherwood number are:

$$Nu_x = \frac{xq_w}{k_{bf}(T_w - T_0)}, \quad Sh_x = \frac{xj_w}{D(C_w - C_0)}, \qquad q_w = -k_{nf}\left(\frac{\partial T}{\partial z}\right)_{z=0}, \quad j_w = -D\left(\frac{\partial C}{\partial z}\right)_{z=0} \tag{14}$$

where $q_w$ ,$j_w$ are the wall heat and mass flux respectively. With the help of transformations, Eqn (14) takes the form,

$$\frac{Nu_x}{\sqrt{Re_x}} = -\theta'(0)\,\phi_5, \quad \frac{Sh_x}{\sqrt{Re_x}} = -\Phi'(0), \tag{15}$$

where $Re_x = a_1 x^2 / \upsilon_{bf}$ , Reynolds number.

## 3. Mathematical Solution

By setting down the PDE Equations (9) through (12) as an initial value problem with boundary conditions, we want to: f = H(1), f' = H(2), f'' = H(3), g = H(4), g' = H(5), g'' = H(6), θ = H(7), θ' = H(8), Φ ' = H(9), Φ "= H(10) and then, we obtain the first-order equation system then it solve through bvp4c Matlab solver.

## 4. Discussion of the findings

By adjusting parameter values, we may examine the fluid effects on velocity, temperature, and concentration profiles. The defined values of the parameters are M=0.2, λ=0.2, $\beta_1 = \beta_2 = 0.1$, S=0.1, Pr=1, $S_1$=0.8, $S_2$=0.8, Sc=0.8, φ=0.05 (nanofluid), and φ=0.0(base fluid). In graphs and tables, the numerical calculations are performed for nanofluid and base fluid (Water) with the various parameters. Table 1 represents the values of properties of nanofluids and base fluid.

*Impact of several parameters on f '(ζ) and g '(ζ) profile*

By amplifying the magnetic parameter, Figure 2 shows that the velocity of fluid tends to decrease, but in Figure 3 velocity of the fluid increases. Moreover, Figure 2 clarifies that the thickness of nanofluid momentum boundary layer is less than the base fluid. Whereas, in Figure 3 boundary layer thickness of base fluid is greater than the nanofluid but by slowly increasing of ζ , the thickness of boundary layer turns vice-versa in a particular value of ζ . With an increment in Maxwell parameter the velocity profile tends to decay and it causes the reduction in momentum boundary layer in Figure 4 and 5. Especially in Figure 5 velocity profile shows cross over point nearly ζ =3 to 4, velocity increases before ζ = 3 and after ζ = 4 velocity starts decreasing. While increasing the rotation parameter, the velocity profile and boundary layer thickness is decayed in Figure 6 and 7. Moreover, the velocity of the fluid decline, but in y-direction, the fluid velocity have some changes after a critical point of x-direction.

*Effect of various parameters on θ (ζ) profile*

The temperature difference for variations of Prandtl number (Pr), thermal stratification parameter ($S_1$) and retardation Deborah number ($\beta_3$) are examined in the Figures 8-10. Higher Pr produces weaker thermal diffusivity of both nanofluid and base fluid which gives degeneration in thermal energy. In Figures 9 and 10, the qualitatively similar effect is noted for different values of $S_1$ and $\beta_3$. By rising the values of $S_1$ and $\beta_3$, temperature sketch and related boundary layer becomes thinner. Physically, due to heat flux model and double stratification, the temperature of the fluid in the surface decreases. Therefore, the temperature distribution decays and as a result boundary layer becomes thinner.

*Impact of various parameters on concentration $\Phi(\zeta)$ profile*

The effects of the solutal stratification ($S_2$) and Schmidt number (Sc) on the $\Phi(\zeta)$ profile is shown in Figures 11 and 12. It is described that the different values of solutal stratification parameter and Schmidt number, reduce the solutal diffusivity sketch as well as the boundary layer thickness also reduced. The thickness of nanofluid concentration boundary is more than the base fluid. This concludes that, when the temperature difference between the wall and surrounding environment grows larger, then the thickness of concentration boundary decreases.

*Effect of several parameters on $Re_x^{-1/2}Nu_x$ and $Re_x^{-1/2}Sh_x$ profile*

The volume proportion of nanoparticles influences the Nusselt number, which determines the rate of heat transmission in the surface. Figure 13 and 14, the heat transfer in Magnetite fluid decreases when the values of rotation rate and retardation number rises, and heat transfer rate rises in Pr and nanoparticle volume fraction with Alumina fluid. The mass transfer rate expressed by the effects of rotation on the Sherwood number in Figure 15. This inspected that the rising of rotation parameter and Schmidt number, which gives decrease in the mass transfer rate with Magnetite nanofluid. For high values of rotation parameter and solutal stratification, the mass transfer rate decreases with nanofluid in Figure 16. Finally, as Pr, $\beta_3$ with nanofluid grows, heat transfer rate increases and thermal boundary layer deepens.

Tables 2 and 3 shows the patterns in heat and mass transmission rates with increasing the several parameters and the Nusselt and Sherwood numbers are compared with different nanofluids and parameters are M=0.2, $\beta_1 = \beta_2 = 0.1$, $\lambda$=0.2, Pr=10, Sc=2.5, S=0.1, $S_1$=0.8, $S_2$=0.8 and $\varphi$=0.05 (nanofluid). According to Table 2, the local Nusselt number's magnitude grows as the Prandtl number increases. When Deborah relaxation number and rotation parameter increases, Nusselt decreases. When the Schmidt number and stretching ratio rise, Table 3 shows a dramatic increase in the local Sherwood number.

## 5. Conclusion

A numerical analysis for rotating Maxwell nanofluid along with magneto-hydrodynamic, non-Fourier heat flux model and double stratification. The numerical method of bvp5c MATLAB algorithm is used to solve the mathematical model. The key observation of this paper is highlighted as below:

- Strong magnetic impact slows the flow rate.

- The fluid velocity is reduced due to enhancement in rotation parameter and Deborah relaxation number. In other words, the cooling process suffers adverse as fluid rotates.
- The temperature gradient diminishes, while rising of Pr, $S_1$ and $\beta_3$.
- Higher values of Sc and $S_2$ are associated with weaker concentration.
- Higher values of the nanoparticle volume fraction with Pr result in an increase in the heat and mass transfer rate; otherwise, the rate degrades.
- In contrast to the temperature and concentration drawing, where the boundary layer thickness of the nanofluid dominates base fluid, the velocity profile shows a thickness of the nanofluid boundary layer that is less than base fluid.

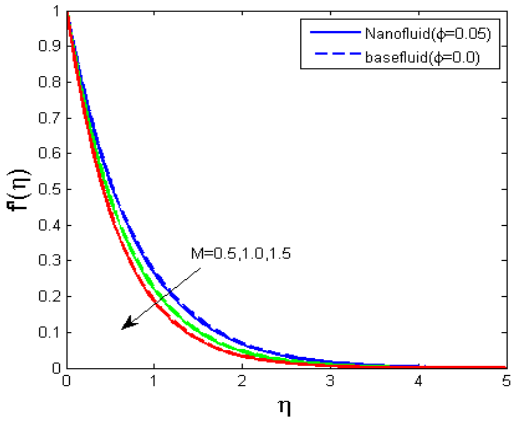


Figure 2: Impact of M on velocity profile

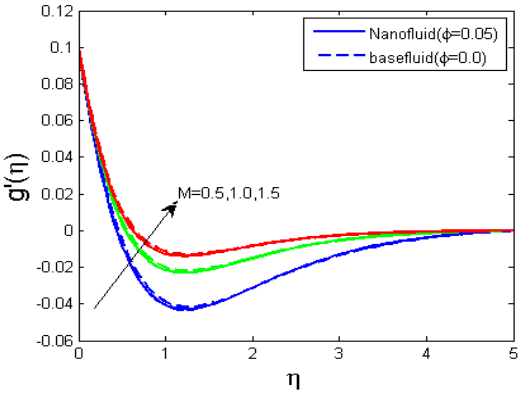


Figure 3: Impact of M on velocity profile

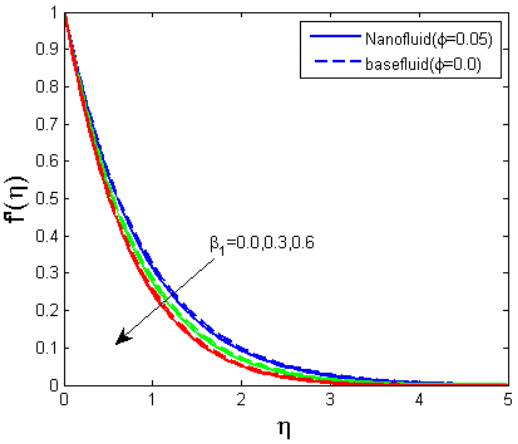


Figure 4: Impact of $\beta_1$ on velocity profile

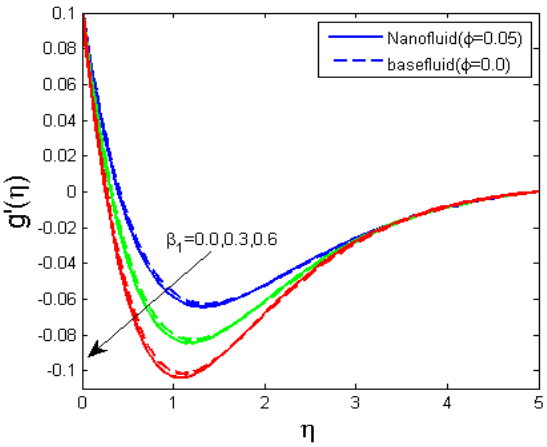


Figure 5: Impact of $\beta_1$ on velocity profile

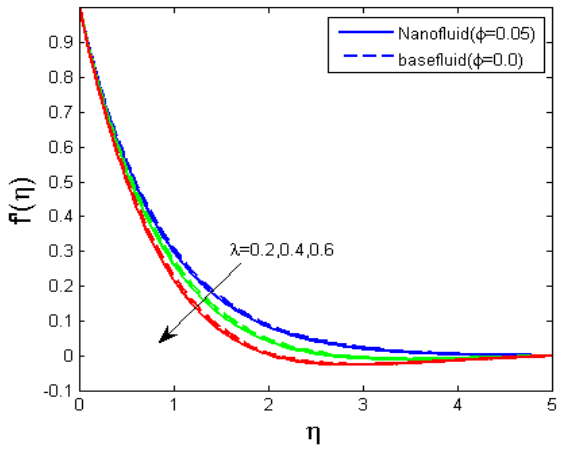


Figure 6: Impact of λ on velocity profile

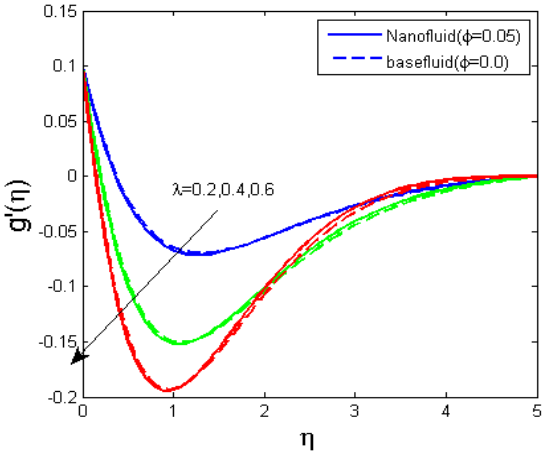


Figure 7: Impact of λ on velocity profile

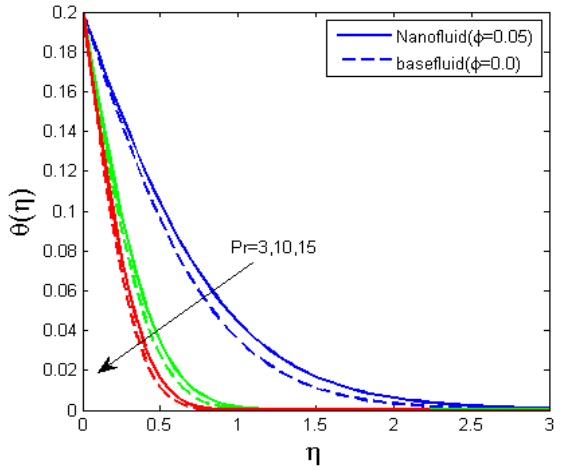


Figure 8: Impact of Pr on temperature profile

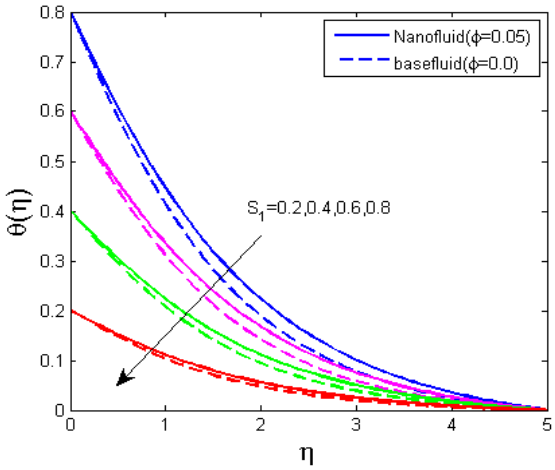


Figure 9: Impact of $S_1$ on temperature profile

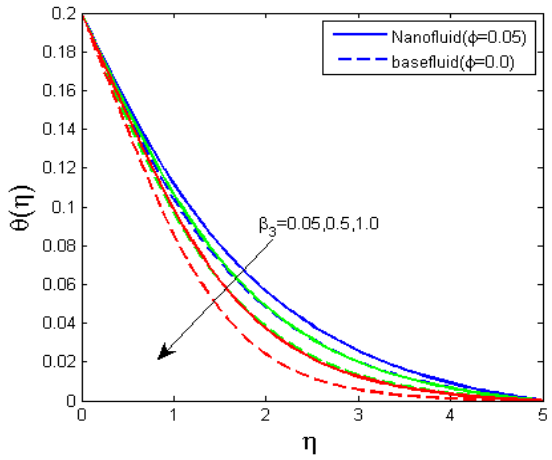


Figure 10: Impact of $\beta_3$ on temperature profile

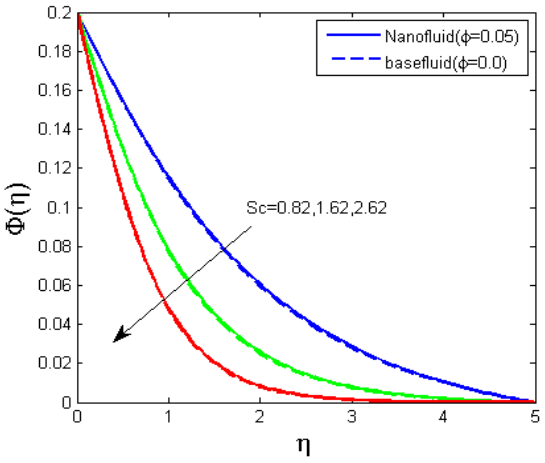


Figure 11: Impact of Sc on Concentration profile

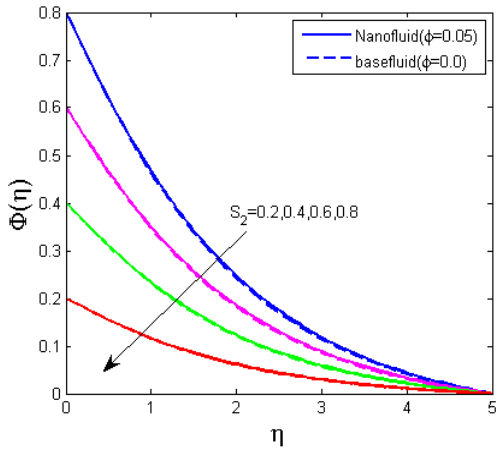


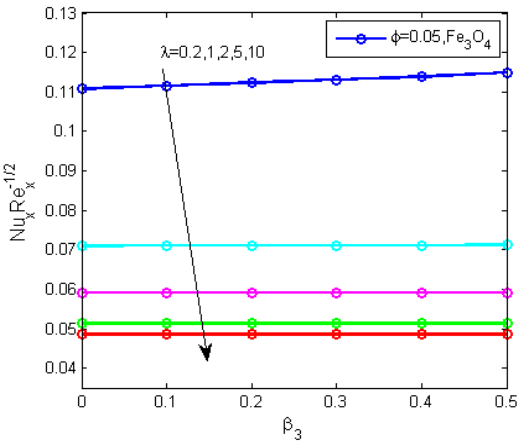


Figure 12: Impact of $S_2$ on Concentration profile. Figure 13: Impact of $\beta_3$ and $\lambda$ on heat transfer rate

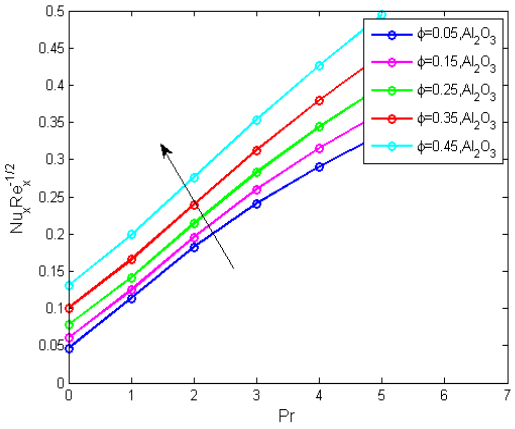


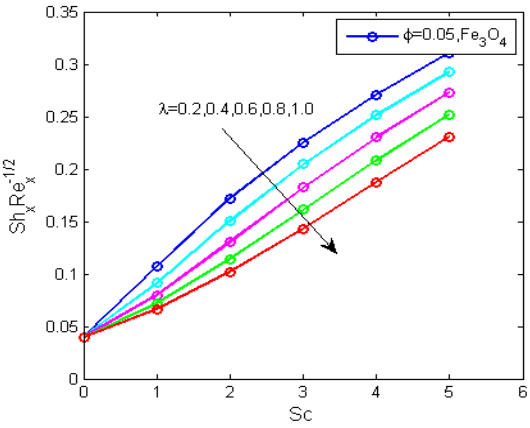


Figure 14: Impact of Pr and φ on heat transfer rate. Figure 15: Impact of Sc and λ on mass transfer rate

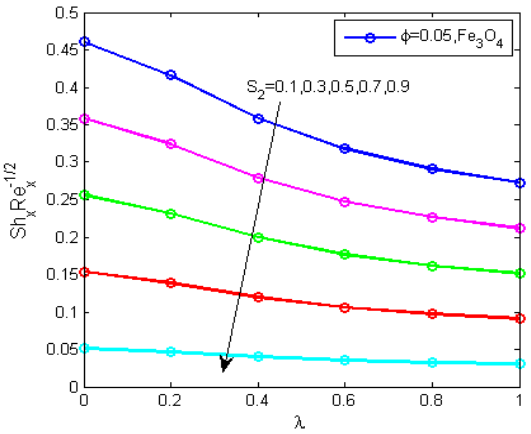


| Properties | $\rho$ $(kg/m^3)$ | $C_p$ $(J/kg\,K)$ | $k$ $(W/m\,K)$ | $\sigma$ $(S/m)$ |
|---|---|---|---|---|
| Water | 997.1 | 4179 | 0.613 | $5.5\text{x}10^6$ |
| Copper | 8933 | 385 | 401 | $59.6\text{x}10^6$ |
| Alumina | 3970 | 765 | 40 | $35\text{x}10^6$ |
| Magnetite | 5180 | 670 | 9.7 | $0.74\text{x}10^5$ |

Figure 16: Impact of S2 and λ on mass transfer rate**Table 1.** Thermophysical properties of nanofluid.

**Table 2** Numerical values of local Nusselt number $-\theta'(0)$ for various values of λ, Pr, β.

| | | | | | $-\theta'(0)$ |
|---|---|---|---|---|---|
| **λ** | **$\beta_1$** | **Pr** | **Cu - Water** | **$Al_2O_3$ - Water** | **$Fe_3O_4$ - Water** |
| 0.1 | 0.1 | 10 | 0.509430 | 0.513045 | 0.509059 |
| 0.2 | | | 0.499952 | 0.505101 | 0.500915 |
| 0.6 | | | 0.456986 | 0.469109 | 0.464188 |
| 0.8 | | | 0.434806 | 0.451455 | 0.446057 |
| | 0.05 | | 0.501755 | 0.506668 | 0.502504 |
| | 0.15 | | 0.498157 | 0.503543 | 0.499334 |
| | 0.25 | | 0.494589 | 0.500455 | 0.496199 |
| | 0.35 | | 0.491044 | 0.497399 | 0.493094 |
| | | 5 | 0.321044 | 0.334080 | 0.330906 |
| | | 10 | 0.499952 | 0.505101 | 0.500915 |
| | | 15 | 0.631682 | 0.635960 | 0.630981 |
| | | 25 | 0.742548 | 0.746134 | 0.740480 |

**Table 3** Numerical values of local Sherwood number $-\Phi'(0)$ for various values of λ, S, Sc.

| | | | | | $-\theta'(0)$ |
|---|---|---|---|---|---|
| **λ** | **S** | **Sc** | **Cu - Water** | **$Al_2O_3$ - Water** | **$Fe_3O_4$ - Water** |
| 0.1 | 0.1 | 10 | 0.204007 | 0.209256 | 0.207933 |
| 0.2 | | | 0.194780 | 0.201603 | 0.199890 |
| 0.6 | | | 0.146775 | 0.159987 | 0.156576 |
| 0.8 | | | 0.127230 | 0.141136 | 0.137444 |
| | 0.2 | | 0.209608 | 0.215819 | 0.214256 |
| | 0.3 | | 0.222392 | 0.228337 | 0.226840 |
| | 0.4 | | 0.233864 | 0.239703 | 0.238233 |
| | 0.5 | | 0.244400 | 0.250222 | 0.248756 |
| | | 5 | 0.305799 | 0.312459 | 0.310793 |
| | | 10 | 0.462331 | 0.468681 | 0.467091 |
| | | 15 | 0.582001 | 0.588198 | 0.586645 |
| | | 25 | 0.682715 | 0.688820 | 0.687288 |

## References

[1] Aamir Ali, M. Sulaiman, S. Islam, Zahir Shah, and Ebenezer Bonyah, Three-dimensional magnetohydrodynamic (MHD) flow of Maxwell nanofluid containing gyrotactic micro-organisms with heat source/sink,AIP Advances 8, 085303 (2018), https://doi.org/10.1063/1.5040540 .

[2] R. Ahmad, M. Mustafa, Model and comparative study for rotating flow of nanofluids due to convectively heated exponentially stretching sheet, Journal of Molecular Liquids, Volume 220, 2016, Pages 635-641, ISSN 0167-7322, https://doi.org/10.1016/j.molliq.2016.04.125 .

[3] Bagh Ali, P.K. Pattnaik, Rizwan Ali Naqvi, Hassan Waqas, Sajjad Hussain, Brownian motion and thermophoresis effects on bio-convection of rotating Maxwell nanofluid over a Riga plate with Arrhenius activation energy and Cattaneo-Christov heat flux theory, Thermal Science and Engineering Progress, 10.1016/j.tsep.2021.100863, 23, (100863), (2021), https://api.semanticscholar.org/CorpusID:234046871 .

[4] Bagh Ali, Thirupathi Thumma, Danial Habib, Nadeem salamat, Saleem Riaz, Finite element analysis on transient MHD 3D rotating flow of Maxwell and tangent hyperbolic nanofluid past a bidirectional stretching sheet with Cattaneo Christov heat flux model, Thermal Science and Engineering Progress, Volume 28, 2022, 101089, ISSN 2451-9049, https://doi.org/10.1016/j.tsep.2021.101089 .

[5] Fouzia Rehman, Muhammad Imran Khan, Muhammad Sadiq, Asad Malook, MHD flow of carbon in micropolar nanofluid with convective heat transfer in the rotating frame, Journal of Molecular Liquids, Volume 231, 2017, Pages 353-363, ISSN 0167-7322, https://doi.org/10.1016/j.molliq.2017.02.022 .

[6] Hassan Waqas, Hamzah Naeem, Umair Manzoor, SivanandamSivasankaran, Ahmad Ayyad Alharbi, Ali Saleh Alshomrani, Taseer Muhammad, Impact of electro-magneto-hydrodynamics in radiative flow of nanofluids between two rotating plates, Alexandria Engineering Journal, Volume 61, Issue 12, 2022, Pages 10307-10317, ISSN 1110-0168, https://api.semanticscholar.org/CorpusID:248031836 .

[7] Hayat Tasawar, Muhammad Taseer, Shehzad, S.A. et al. Three-dimensional boundary layer flow of Maxwell nanofluid: mathematical model. Appl. Math. Mech.-Engl. Ed. 36, 747–762 (2015), https://doi.org/10.1007/ s10483-015-1948-6 .

[8] Iskander Tlili, Sania Naseer, Muhammad Ramzan, Seifedine Kadry, and Yunyoung Nam, Effects of chemical species and nonlinear thermal radiation with 3D Maxwell nanofluid flow with double stratification - An analytical solution, Journal of Entropy, 2020, 22(4), 453, doi:10.3390/e22040453.

[9] M. Mustafa, Tasawar Hayat, Ahmed Alsaedi, Rotating flow of Maxwell fluid with variable thermal conductivity: An application to non-Fourier heat flux theory, International Journal of Heat and Mass Transfer, 106 (2017), 142-148, https://doi.org/10.1016/j.ijheatmasstransfer.2016.10.051.

[10] Muhammad Awais, Najeeb Ullah, Javaid Ahmad, Faizan Sikandar, Mohammad Monjurul Ehsan, SayedusSalehin, Arafat A. Bhuiyan, Heat transfer and pressure drop performance of Nanofluid: A state-of- the-art review, International Journal of Thermofluids, Volume 9, 2021, 100065, ISSN 2666-2027, https://doi.org/10.1016/j.ijft.2021.100065.

[11] Muhammad Naveed Khan, Sohail Nadeem, A comparative study between linear and exponential stretching sheet with double stratification of a rotating Maxwell nanofluid flow, Surfaces and Interfaces, Volume 22, 2021, 100886, ISSN 2468-0230, https://doi.org/10.1016/j.surfin.2020.100886.

[12] Qiu-Hong Shi, Muhammad Naveed Khan, Nadeem Abbas, M. Ijaz Khan and Faris Alzahrani, Heat and mass transfer analysis in the MHD flow of radiative Maxwell nanofluid with non-uniform heat source/sink, Waves in Random and Complex Media, 2021, 1-24, https://api.semanticscholar.org/CorpusID:244265178.

[13] Rahimah Jusoh, Roslinda Nazar, Ioan Pop, Flow and Heat Transfer of Magnetohydrodynamic ThreeDimensional Maxwell Nanofluid over a Permeable Stretching/Shrinking Surface with Convective Boundary Conditions, International Journal of Mechanical Sciences S0020-7403(16), 31010-4, https://doi.org/10. 1016/j.ijmecsci.2017.02.022.

[14] KD Ramaiah, P S, G. Kotha, K. Thangavelu, MHD rotating flow of a Maxwell fluid with Arrhenius activation energy and non-Fourier heat flux model. Heat Transfer, 2020, 1-19, https://api.semanticscholar.org/CorpusID:216402879.

[15] Sadia Rashid, M. Ijaz Khan, Tasawar Hayat, M. Ayub, Ahmed Alsaedi, Numerical treatment for rotating Maxwell nanomaterial flow with Arrhenius energy, Applied Nano science, 10, pages 2665–2672 (2020), https://doi.org/10.1007/s13204-019-00998-3.

[16] M. Sheikholeslami, M. Hatami, D.D. Ganji, Nanofluid flow and heat transfer in a rotating system in the presence of a magnetic field, Journal of Molecular Liquids, Volume 190, 2014, Pages 112-120, ISSN 0167-7322, https://doi.org/10.1016/j.molliq.2013.11.002.

[17] Tariq Hussain, Shafqat Hussain, Tasawar Hayat, Impact of double stratification and magnetic field in mixed convective radiative flow of Maxwell nanofluid, Journal of Molecular Liquids, Volume 220, 2016, Pages 870-878, ISSN 0167-7322, https://doi.org/10.1016/j.molliq.2016.05.012.

[18] Tasawar Hayat, Taseer Muhammad, M. Mustafa, A. Alsaedi, An optimal study for three-dimensional flow of Maxwell nanofluid subject to rotating frame,Journal of Molecular Liquids, Volume 229, 2017, Pages 541-547, ISSN 0167-7322, https://doi.org/10.1016/j.molliq.2017.01.005.

[19] Tasawar Hayat, Arsalan Aziz, Taseer Muhammad, Ahmed Alsaedi, Effects of Binary chemical reaction and Arrhenius activation energy in Darcy-Forchheimer three-dimensional flow of nanofluid subject to rotating frame, Journal of Thermal Analysis and Calorimetry , 136, 1769 - 1779 (2019),https://doi.org/10.1007/s10973-018-7822-6.

[20] Tasawar Hayat, Arsalan Aziz, Taseer Muhammad, Ahmed Alsaedi, Numerical simulation for DarcyForchheimer three-dimensional rotating flow of nanofluid with prescribed heat and mass flux conditions, Journal of Thermal Analysis and Calorimetry, 136, 2087 - 2095 (2019), https://doi.org/10.1007/s10973-018-7847-x.

[21] Tasawar Hayat, Sajid Qayyum, Sabir Ali Shehzad, Ahmed Alsaedi, Cattaneo-Christov double-diffusion theory for three-dimensional flow of viscoelastic nanofluid with the effect of heat generation/absorption,Results in Physics, Volume 8,2018, Pages 489-495, ISSN 2211-3797,https://doi.org/10.1016/j.rinp.2017.12.060.

[22] Tasawar Hayat, Taseer Muhammad, S.A. Shehzad, A. Alsaedi, Three dimensional rotating flow of Maxwell nanofluid, Journal of Molecular Liquids, Volume 229, 2017, Pages 495-500, ISSN 0167-7322,https://doi.org/10.1016/j.molliq.2016.12.095.

[23] F. Wang, S. Ahmad, Q. Al Mdallal, et al. Natural bio-convective flow of Maxwell nanofluid over an exponentially stretching surface with slip effect and convective boundary condition. Scientific Reports 12, 2220 (2022), DOI:10.1038/s41598-022-04948-y.

[24] Wasim Jamshed, Numerical investigation of MHD impact on Maxwell Nanofluid, International Communications in Heat and Mass Transfer, 120 (2021) 104973,https://doi.org/10.1016/j.icheatmasstransfer.2020.104973.

[25] Yu-Ming Chu, Muhammad Ramzan, Naila Shaheen, Jae Dong Chung, Seifedine Kadry, Fares Howari, M.Y. Malik, Hassan Ali S. Ghazwani, Analysis of Newtonian heating and higher-order chemical reaction on a Maxwell nanofluid in a rotating frame with gyrotactic microorganisms and variable heat source/sink, Journal of King Saud University - Science, Volume 33, Issue 8, 2021, 101645, ISSN 1018-3647, https://doi.org/10.1016/j.jksus.2021.101645.

[26] Z. Shafique, M. Mustafa, A. Mushtaq, Boundary layer flow of Maxwell fluid in rotating frame with binary chemical reaction and activation energy,Results in physics, 6 (2016), 627 – 633,https://api.semanticscholar.org/CorpusID:99113502.

[27] Shampine, L. F., Kierzenka, J. Reichelt, M. W. Solving boundary value problems for ordinary differential equations in MATLAB with bvp4c.Tutorial Notes, 1–27 (2000), https://api.semanticscholar.org/CorpusID:427544.